Cell culture-grown hepatitis C virus is infectious *in vivo* and can be recultured *in vitro*

Brett D. Lindenbach*†, Philip Meuleman†‡, Alexander Ploss*, Thomas Vanwolleghem‡, Andrew J. Syder*, Jane A. McKeating§, Robert E. Lanford¶, Stephen M. Feinstone‖, Marian E. Major‖, Geert Leroux-Roels‡, and Charles M. Rice*,**

*Center for the Study of Hepatitis C, Laboratory of Virology and Infectious Disease, The Rockefeller University, 1230 York Avenue, New York, NY 10021; ‡Center for Vaccinology, Ghent University and Hospital, Building A, First Floor, De Pintelaan 185, 9000 Ghent, Belgium; §Division of Immunity and Infection, Institute of Biomedical Research, University of Birmingham Medical School, Birmingham B15 2TT, United Kingdom; ¶Department of Virology and Immunology, Southwest National Primate Research Center and Southwest Foundation for Biomedical Research, 7620 NW Loop 410, San Antonio, TX 78245; and ‖Laboratory of Hepatitis Viruses, Division of Viral Products, Center for Biologics Evaluation and Research, Food and Drug Administration, 8800 Rockville Pike, Bethesda, MD 20892

Hepatitis C virus (HCV) is a major cause of chronic liver disease, frequently progressing to cirrhosis and increased risk of hepatocellular carcinoma. Current therapies are inadequate and progress in the field has been hampered by the lack of efficient HCV culture systems. By using a recently described HCV genotype 2a infectious clone that replicates and produces infectious virus in cell culture (HCVcc), we report here that HCVcc strain FL-J6/JFH can establish long-term infections in chimpanzees and in mice containing human liver grafts. Importantly, virus recovered from these animals was highly infectious in cell culture, demonstrating efficient *ex vivo* culture of HCV. The improved infectivity of animal-derived HCV correlated with virions of a lower average buoyant density than HCVcc, suggesting that physical association with low-density factors influences viral infectivity. These results greatly extend the utility of the HCVcc genetic system to allow the complete *in vitro* and *in vivo* dissection of the HCV life cycle.

animal model | pathogenesis | reverse genetics | viral hepatitis

A major limitation in hepatitis C virus (HCV) research has been the lack of virus culture systems. After identification of the viral genome in 1989 (1), early efforts focused on understanding the structure and function of individual viral gene products. HCV is an enveloped, positive-strand RNA virus classified in the family *Flaviviridae* (2). The 9.6-kb ssRNA genome encodes three structural (virion-associated) and seven nonstructural (intracellular) genes within a single ORF.

The first functional cDNA clones of HCV were constructed in 1997, allowing chimpanzees to be infected after intrahepatic transfection with recombinant viral RNA (3, 4). Unfortunately, these infectious genomes failed to replicate in cell culture. By engineering HCV replicons to express a drug-selectable gene, it became possible to select for HCV RNA replication in cell culture (5). However, efficient replication required cell culture-adaptive mutations in the viral RNA (6). Moreover, only the intracellular aspects of HCV replication were modeled by these systems. For unknown reasons, cell culture-adaptive mutations can inhibit virion production in culture (T. Pietschmann and R. Bartenschlager, personal communication) and attenuate RNA infectivity *in vivo* (7).

Recent progress in the field has come from the identification of JFH-1, a genotype 2a subgenomic replicon that does not require adaptive mutations for efficient RNA replication in culture (8). Based on this sequence, we constructed a chimeric JFH-1 genome containing the core to nonstructural protein 2 (NS2) region of HCV strain J6. This genome, FL-J6/JFH, replicated and produced high levels of infectious virus in cell culture (HCVcc) (9), allowing us to study new aspects of the viral life cycle in tissue culture (9, 10). Similarly, full-length JFH-1 clones produced HCVcc, albeit with delayed kinetics of virus release (11, 12). HCVcc strain JFH-1 was able to transiently infect a chimpanzee, although replication levels were low and did not induce an immune response (11). To further extend the utility of the HCVcc system, we examined the ability of FL-J6/JFH to infect chimpanzees and chimeric urokinase-type plasminogen activator (uPA)–severe combined immunodeficiency (SCID) mice, as well as the characteristics of recovered virus in cell culture.

Results

HCVcc Is Infectious in Chimpanzees. We investigated whether HCVcc strain FL-J6/JFH would be infectious *in vivo* by inoculating two HCV-negative chimpanzees via i.v. injection with 1×10^6 tissue culture infectious doses (50% endpoint, TCID$_{50}$). Both animals exhibited a rapid rise in viremia, peaking between 10^4 and 10^5 international units (IU) of HCV RNA per ml of plasma within 2 weeks postinfection (Fig. 1*A*). After an acute viremic phase, the viral load in chimpanzee 4x0483 decreased but was maintained between 10^2 and 10^4 IU/ml for 17 weeks before dropping below the limit of detection. In contrast, the viral load in chimpanzee 4x0495 became undetectable by week 7 then reappeared briefly at week 15. Neither animal exhibited clinical signs of hepatitis or elevated serum alanine aminotransferase (ALT) and aspartate aminotransferase (AST) throughout 4 months of observation (Fig. 1*A*). These data demonstrate that HCVcc is capable of establishing infection *in vivo* and that the virus can persist in these animals for at least several weeks.

The decrease and fluctuations in viremia are consistent with previously observed patterns of acute HCV infection that are then controlled by innate and adaptive immune responses (13). Consistent with this, both chimpanzees developed HCV-specific humoral responses at weeks 10 and 13 (Fig. 1*B*). We also measured the induction of intrahepatic cell-mediated and innate host responses of these animals by measuring the relative CD3ε, IFN-γ, and 2′,5′-oligoadenylate synthetase 1 (OAS1) mRNA levels in liver biopsy samples. The induction of CD3ε and IFN-γ indicated that T and/or natural killer cells were recruited and activated within the livers of both HCVcc-infected chimpanzees (Fig. 1*C*). Consistent with this, infiltrating lymphocytes were found within liver biopsies from both chimpanzees (Fig. 4, which
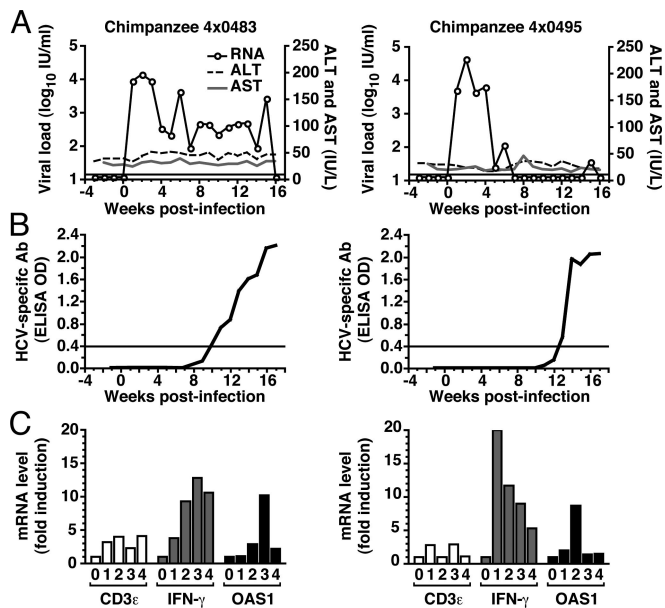
Fig. 1. HCVcc is infectious in chimpanzees. (*A*) HCV RNA viral load (open circles) was measured in the weekly serum or plasma of each animal (see *Methods*) and expressed as World Health Organization IU per ml. Serum levels of ALT (dashed line) and AST (gray line), measured at each time point, are expressed as IU/liter. (*B*) HCV-specific antibody levels were quantitated by a standard HCV-diagnostic ELISA (see *Methods*) and expressed as optical density (OD) units. The cutoff for a positive reaction was 0.4 OD. (*C*) Liver biopsies were taken at 0, 1, 2, 3, and 4 months postinfection. The relative levels of CD3ε, IFN-γ, and OAS1 mRNAs, quantitated and normalized to the levels at month 0 (see *Methods*), are expressed as the fold induction.

Fig. 2. HCVcc is infectious in chimeric uPA-SCID mice. Viral loads (open circles) and levels of human albumin (dashed line) were quantitated (see *Methods*) in the plasma from mice infected with HCV-J4 (*A*), HCVcc strain FL-J6/JFH (*B* and *C*), or plasma from mouse C (*D*). Mice A and B were killed at 5 weeks postinfection, and mouse C was killed at 14 weeks postinfection. The limit of HCV RNA detection is indicated by a horizontal bar.

is published as supporting information on the PNAS web site). Furthermore, the increased expression of OAS1 mRNA indicated that intrahepatic type 1 IFN responses were induced in both animals (Fig. 1*C*). Taken together, these data demonstrate that innate and acquired immune responses were targeted to the liver in both HCVcc-infected animals.

HCVcc Is Infectious in uPA-SCID Mice Containing Human Hepatocytes. We also examined the infectivity of HCVcc in one of the few small animal models for HCV infection, uPA-SCID mice transplanted with human hepatocytes (14, 15). As a positive control, mouse A was infected by a reference strain of HCV, HC-J4, and reached titers of 10^5 IU/ml (Fig. 2*A*). Within 2 weeks after infection with HCVcc, plasma from mice B and C contained high levels of HCV RNA, between 10^6 and 10^7 IU/ml, and viral loads remained above 10^5 IU/ml in both animals until they were killed at weeks 5 and 14, respectively (Fig. 2 *B* and *C*). Importantly, HCV RNA remained undetectable in an uninfected uPA$^{+/+}$-SCID chimeric mouse and in an HCVcc-inoculated uPA$^{+/-}$-SCID mouse that did not receive human hepatocytes (data not shown). After inoculation with 5 μl of week-3 plasma from mouse C, mouse D became infected and supported a high viral load for over 17 weeks (Fig. 2*D*). Plasma levels of human albumin were used to assess the function of transplanted human hepatocytes and were within normal ranges (15). These data further demonstrate that HCVcc is infectious *in vivo* and show that infection can be serially passed to a naïve animal.

Virus Recovered from Infected Animals Is Infectious in Cell Culture. There have been no reliable methods to culture clinical isolates of HCV to date. We therefore investigated whether HCV present in the plasma and sera from HCVcc-infected animals was infectious in cell culture. Measurable levels of infectivity
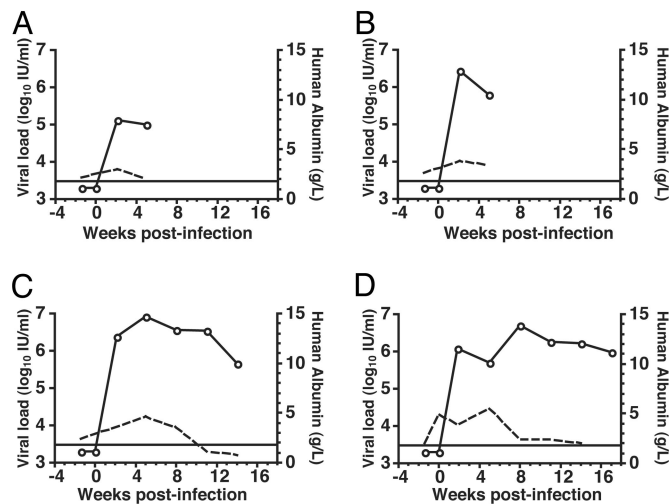
were found in two separate samples from each chimpanzee, and high levels of infectivity were measured in plasma taken from mice C and D at weeks 3 and 17, respectively (Table 1). HC-J4 infectivity was not detected in plasma from mouse A, which is consistent with the exceptional ability of JFH-derived viruses to grow in cell culture. Because mouse D had been inoculated with plasma from mouse C at week 3, the FL-J6/JFH virus present in this animal had spent 20 weeks *in vivo*. Thus, the chimeric FL-J6/JFH genome retained *in vitro* infectivity even after prolonged growth *in vivo*.

Characterization of the Virus Recovered from HCVcc-Infected Animals. Sequencing of the NS2-3 junction region amplified by RT-PCR confirmed that animals were infected with FL-J6/JFH. To further examine infectivity, we quantified the specific infectivity in samples derived from HCVcc-infected animals. The calculation of specific infectivity normalizes the amount of infectivity to the amount of viral RNA present in a virus preparation (9). Of note, the specific infectivity values of animal-derived viruses were much higher than that of HCVcc (Table 1). After culture in Huh-7.5 cells, animal-derived HCV isolates again exhibited lower specific infectivity (Table 1), suggesting that HCV grown *in vivo* was more infectious than HCV grown in cell culture.

To characterize possible physical differences between HCV grown *in vitro* and *in vivo*, we measured the buoyant densities of HCV RNA-containing particles in equilibrium gradients. HCVcc exhibits a broad distribution of buoyant density, with a peak of viral RNA at 1.14 g/ml but a peak of specific infectivity at 1.10 g/ml (9). Consistent with these previous results, a major peak of HCVcc RNA was observed at 1.14 g/ml, with smaller amounts of viral RNA present at the top of the gradient (Fig. 3*A*). In contrast, HCV RNA present in chimpanzee 4x0483 plasma at 3 weeks postinfection exhibited a major peak at 1.10 g/ml and a smaller peak at 1.14 g/ml (Fig. 3*B*). After passage of this virus in cell culture, the major peak of buoyant density was found at 1.13 g/ml, with a smaller peak near the top of the gradient (Fig. 3*C*). Similar results were obtained for chimpanzee 4x0495 and mouse D (Fig. 5, which is published as supporting information on the PNAS web site). Taken together, these results indicate that the shift to lower buoyant density correlated with the increased specific infectivity of HCV grown *in vivo*.

Table 1. Recovery of cell culture infectivity from HCVcc-infected animals

Virus preparation	Time in vivo, weeks	Time in vitro, days	Infectivity, $TCID_{50}/ml$	Specific infectivity, $TCID_{50}$ per RNA
FL-J6/JFH (HCVcc)	n/a*	5.7 ± 2.3	3.93×10^4 ($\pm 2.63 \times 10^4$)	1/1,230 ($\pm 1/602$)
Viruses present in vivo				
Chimpanzee 4×0483	1	n/a	6.26×10^2	1/15
	3	n/a	1.92×10^2	1/50
Chimpanzee 4×0495	2	n/a	3.00×10^2	1/148
	3	n/a	1.75×10^2	1/25
Mouse A	3	n/a	<10	n/a
Mouse C	3	n/a	6.93×10^4	1/9
Mouse D	20	n/a	5.38×10^4	1/18
Viruses recovered in vitro				
Chimpanzee 4×0483	3	9	2.43×10^3	1/1,090
Chimpanzee 4×0495	3	9	7.94×10^3	1/1,260
Mouse D	20	5	5.38×10^5	1/472

n/a, not applicable. *Average values from seven independent stocks of HCVcc (±SD).

Discussion

Our results show that the chimeric HCVcc strain FL-J6/JFH is infectious in vivo and can persist in infected animals for several weeks. HCV was detected in chimpanzee 4x0483 up to 15 weeks, whereas chimpanzee 4x0495 showed transient clearance at week 7 followed by reappearance of virus at week 15. Importantly, both animals developed HCV-specific antibodies and showed evidence of intrahepatic immune responses (Fig. 1). HCVcc strain FL-J6/JFH also produced robust infections in chimeric uPA-SCID mice that persisted for at least 14 weeks and could be passed to another animal (Fig. 2). Previously, Wakita and colleagues (11) showed that full-length JFH-1 HCVcc could infect a chimpanzee, although viremia was ≈100-fold lower than what we observed, HCV-specific antibodies did not develop, and virus became undetectable after 4 weeks. These discrepancies could reflect differences between virus strains, doses used for infection, or host responses to infection. In the present study, viremia peaked early at 2 weeks postinfection. Notably, IFN-γ mRNA was rapidly induced in both chimpanzees, and the animal with the stronger and earlier IFN-γ response, 4x0495, was more effective in controlling the infection. These data are consistent with a critical role for IFN-γ in HCV clearance (16, 17). However, the late induction of OAS at 2 to 3 months postinfection differed from what has been previously observed during infection of naïve chimpanzees. We cannot rule out the possibility that OAS may have been transiently induced before the first biopsy samples at 1 month postinfection. Alternatively, the rapid production of IFN-γ may have blunted the type I IFN response during the early acute phase, as has been observed for hepatic cells in vitro (18). Furthermore, in chimeric uPA-SCID mice, which lack functional immune responses, HCV replication continued unabated. The lack of detectable changes in chimpanzee ALT and AST, which has also been observed in other

HCV-infected chimpanzees (7, 16, 17), indicates that few hepatocytes were destroyed. This finding is likely to reflect a complex association between the rate of cell death, percentage of cells infected, and potential noncytolytic clearance mechanisms. Further work is necessary to determine how viral and host determinants contribute to the outcome of disease.

Unlike most clinical isolates of HCV, FL-J6/JFH viruses grown in vivo could be isolated from infected animals and recultured in vitro. Our data demonstrate that the ability to grow in cell culture is stably maintained in the virus population even after 20 weeks in vivo. Indeed, the virus recovered from these animals had higher specific infectivity than virus grown in cell culture (Table 1). Previous estimates of HCV-specific infectivity, based on the measurement of chimp infectious doses, ranged from 1/10 to 1/1,000 (19, 20). Low specific infectivity values have also been described for other positive-strand RNA viruses, such as picornaviruses (21) and flaviviruses (W. Wahala and A. de Silva, personal communication) and likely reflect the overproduction of immature or defective virus particles as well as inefficiencies at early steps in the virus life cycle. We therefore looked at the physical properties of HCV grown in vitro and in vivo and found that a majority of cell culture-derived HCV particles had a buoyant density near 1.14 g/ml, whereas animal-derived HCV particles had a peak buoyant density ≤1.10 g/ml (Figs. 3 and 5). Consistent with this, HCVcc with the highest specific infectivity was previously shown to have a buoyant density of 1.10 g/ml (9). Similarly, clinical isolates of HCV with a high specific infectivity in animals were found to have buoyant densities ≤1.09 g/ml (22). These observations could reflect increased in vivo formation of infectious low-density virions or rapid turnover of poorly infectious, high-density virions. Although it is possible that genetic changes within the viral genome influenced the observed differences in buoyant density, we feel
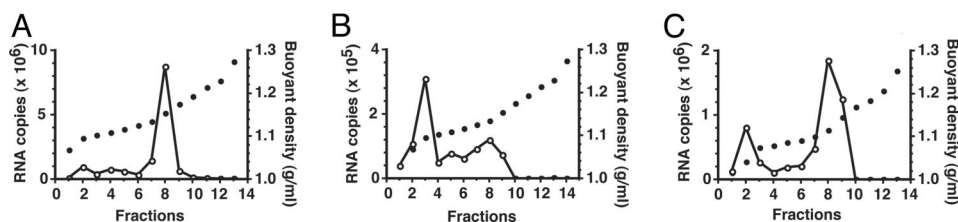
Fig. 3. HCV grown in vivo has a lower buoyant density than HCV grown in vitro. The relative viral RNA levels (open circles) and buoyant density (filled circles) were plotted for each fraction. Gradients were loaded with HCVcc (A), plasma from chimpanzee 4x0483 at 3 weeks postinfection (B), and virus recovered from chimpanzee 4x0483 week 3, then passaged in cell culture for 9 days (C). Fraction 1 corresponds to the top of each gradient.

that genetic changes alone are unlikely to account for the improved specific infectivity because animal-derived viruses quickly returned to lower specific infectivity and higher average buoyant density after culture *in vitro*. Although the biochemical and genetic differences between high- and low-density HCV particles are not yet fully understood, it is known that HCV can associate with β-lipoproteins (23) and that high-density lipoproteins facilitate HCV-glycoprotein-mediated virus entry (24–26). Taken together, these data indicate that the improved infectivity of HCV produced *in vivo* may be due to increased association with lipoproteins or other modification to the virion.

In summary, we have shown that HCVcc is capable of sustained replication in two animal models and that virus recovered from these animals remains infectious in cell culture. The ability to study a genetically defined virus *in vitro* and *in vivo* now allows the determinants of HCV infectivity, pathogenesis, neutralization, and immune escape to be dissected at the molecular level. Furthermore, these results show that it should be possible to culture HCV from clinical samples and provide a useful positive control to help isolate additional strains that grow in cell culture.

Methods

Chimpanzees. Chimpanzees were housed at the Southwest National Primate Research Center at the Southwest Foundation for Biomedical Research and cared for by members of the Department of Comparative Medicine in accordance with the Guide for the Care and Use of Laboratory Animals. All protocols were approved by the Institutional Animal Care and Use Committee. Both animals had been previously used for other studies. Chimpanzee 4x0483 (b. 2/26/1984) was infected with hepatitis E virus in 1988 and HIV in 1998, and received pooled human serum in 1989 that was from a patient with chronic hepatitis of unknown origin. This patient was diagnosed with chronic non-A, non-B, hepatitis based on 36 months of elevated liver enzymes and was negative for anti-HCV antibodies as determined by using the first-generation ELISA. Chimpanzee 4x0495 (b. 1/1/1968) was repeatedly immunized (10 times) with purified hepatitis B virus surface antigen in 1985 and inoculated with HIV in 1994. In 1996, while at a different primate center, this animal received an unspecified injection. No records are available on this procedure. At the beginning of our study, neither chimpanzee had detectable HCV RNA (see below) or an HCV-specific antibody response. Chimpanzees were infected by i.v. injection with 10^6 TCID$_{50}$ of virus in 1 ml on 5/24/2005. Blood was collected weekly. HCV-specific antibodies were measured with ELISA Testing System 3.0 (Ortho Diagnostic Systems). Serum ALT and AST levels were measured by using an automated clinical analyzer.

Mice. All mouse studies were conducted at the Ghent University Hospital, with protocols approved by the Ethical Committee and Animal Ethics Committee of the Ghent University Faculty of Medicine. Transgenic mice that overexpress the uPA gene under the control of an albumin promoter readily accept foreign hepatocytes due to the degeneration of endogenous hepatocytes (14, 15, 27). By combining the uPA$^{+/+}$ and SCID background, which prevents xenograft rejection, mice can be repopulated with human hepatocytes. Homozygous uPA$^{+/+}$-SCID mice were produced by crossing B6SJL-TgN(Alb1Plau)144Bri and CBySmn.CB17-*Prkdc^scid^* mice purchased from the Jackson Laboratory, as described in ref. 15. Genotyping of the uPA-SCID mice was performed via a multiplex PCR as described in ref. 28. The SCID phenotype was confirmed by using an in-house mouse IgM sandwich ELISA. Human hepatocytes were isolated from an HCV-negative patient undergoing partial hepatectomy for the resection of metastatic disease. This patient gave written, informed consent. Around 1 million hepatocytes were used to repopulate the liver of 6- to 14-day-old uPA$^{+/+}$-SCID mice, as described in ref. 15. HCVcc-infected mice were inoculated by intrasplenic injection with 5×10^4 TCID$_{50}$ (RNA copies = 1.04×10^8 IU) in 50 μl. HC-J4-infected mice were inoculated similarly with 1.25×10^6 IU in 25 μl.

Viruses. FL-J6/JFH was grown in Huh-7.5 cells as described in ref. 9. The HCVcc stock used to infect chimpanzees was prepared by concentration in an Amicon Ultra-15 100,000 MWCO ultrafiltration device (Millipore) according to the manufacturer's instructions. HCVcc used to infect chimeric uPA-SCID mice was concentrated by two rounds of polyethylene glycol precipitation (9) and resuspended to 1×10^6 TCID$_{50}$/ml in standard growth media. Plasma from a chimeric uPA-SCID mouse infected with strain HC-J4 (15) served as a positive control for mouse infectivity. Viruses were titered as described in ref. 9, except that serial 2- or 3-fold dilutions were used to titer viruses present in plasma or serum. To prevent clotting of plasma samples, heparin was added at 1 United States Pharmacopoeia unit/ml. Control experiments indicated that this level of heparin only moderately (<3-fold) inhibited HCVcc titers.

RNA Quantitation. All HCV viral loads present in plasma, sera, and tissue culture media were determined by using the COBAS AmpliPrep/COBAS TaqMan HCV assay (Roche Diagnostics), which has a detection limit of 15 World Health Organization IU per reaction. For mouse samples, the limit of detection in 5 μl of plasma was therefore 3×10^3 IU. HCV RNAs were extracted from buoyant density gradient fractions by using the QIAamp Viral RNA mini kit (Qiagen) and quantitated by using an in-house TaqMan assay as described in ref. 9. The sensitivity of this assay was ≈100 RNA copies per reaction, and it should be noted that 1 IU in the Roche AmpliPrep HCV assay corresponds to 10.8 RNA copies in our in-house assay. The relative induction levels of specific mRNAs within liver biopsies were determined as described in ref. 16. In brief, the arithmetic operation $2^{\Delta\Delta CT}$ was used to calculate the amount of target normalized to an endogenous reference (GAPDH) and relative to a calibrator (a liver biopsy taken before challenge), where ΔC_T is the difference between the threshold cycles for a target mRNA and an endogenous reference (GAPDH) mRNA, and $\Delta\Delta C_T$ is the difference between the ΔC_T values of the target mRNA before and after challenge.

Equilibrium Gradients. Gradients were formed with 10–40% iodixanol, essentially as described in ref. 9. However, because of the low level of RNA present in chimpanzee 4x0483 plasma, this gradient was formed from 10% and 40% iodixanol solutions mixed with 8 ml of plasma, total. Preliminary experiments indicated that identical results were obtained by loading HCVcc at the top, at the bottom, or distributed throughout gradients. Nevertheless, for appropriate comparison (Fig. 3 *A* and *B*), a parallel gradient was formed from iodixanol mixed with HCVcc diluted 1:100 in 10 mM Hepes (pH 7.55), 150 mM NaCl, and 0.02% (wt/vol) BSA. All other samples were loaded by overlaying onto preformed gradients. Gradients were run to equilibrium for 6 h at 4°C and 40,000 rpm (197,000 × g_{av}). Depending on the volume loaded, 12–14 fractions were collected from the bottom of the gradient after tube puncture with a fraction collection system (Beckman Coulter). Buoyant densities were determined by refractometry on an Abbé 3L refractometer (Bausch & Lomb).

1. Choo, Q. L., Kuo, G., Weiner, A. J., Overby, L. R., Bradley, D. W. & Houghton, M. (1989) *Science* **244,** 359–362.
2. Lindenbach, B. D. & Rice, C. M. (2005) *Nature* **436,** 933–938.
3. Kolykhalov, A. A., Agapov, E. V., Blight, K. J., Mihalik, K., Feinstone, S. M. & Rice, C. M. (1997) *Science* **277,** 570–574.
4. Yanagi, M., Purcell, R. H., Emerson, S. U. & Bukh, J. (1997) *Proc. Natl. Acad. Sci. USA* **94,** 8738–8743.
5. Lohmann, V., Korner, F., Koch, J., Herian, U., Theilmann, L. & Bartenschlager, R. (1999) *Science* **285,** 110–113.
6. Blight, K. J., Kolykhalov, A. A. & Rice, C. M. (2000) *Science* **290,** 1972–1974.
7. Bukh, J., Pietschmann, T., Lohmann, V., Krieger, N., Faulk, K., Engle, R. E., Govindarajan, S., Shapiro, M., St. Claire, M. & Bartenschlager, R. (2002) *Proc. Natl. Acad. Sci. USA* **99,** 14416–14421.
8. Kato, T., Date, T., Miyamoto, M., Furusaka, A., Tokushige, K., Mizokami, M. & Wakita, T. (2003) *Gastroenterology* **125,** 1808–1817.
9. Lindenbach, B. D., Evans, M. J., Syder, A. J., Wolk, B., Tellinghuisen, T. L., Liu, C. C., Maruyama, T., Hynes, R. O., Burton, D. R., McKeating, J. A. & Rice, C. M. (2005) *Science* **309,** 623–626.
10. Tscherne, D. M., Jones, C. T., Evans, M. J., Lindenbach, B. D., McKeating, J. A. & Rice, C. M. (2006) *J. Virol.* **80,** 1734–1741.
11. Wakita, T., Pietschmann, T., Kato, T., Date, T., Miyamoto, M., Zhao, Z., Murthy, K., Habermann, A., Krausslich, H. G., Mizokami, M., *et al.* (2005) *Nat. Med.* **11,** 791–796.
12. Zhong, J., Gastaminza, P., Cheng, G., Kapadia, S., Kato, T., Burton, D. R., Wieland, S. F., Uprichard, S. L., Wakita, T. & Chisari, F. V. (2005) *Proc. Natl. Acad. Sci. USA* **102,** 9294–9299.
13. Bowen, D. G. & Walker, C. M. (2005) *Nature* **436,** 946–952.
14. Mercer, D. F., Schiller, D. E., Elliott, J. F., Douglas, D. N., Hao, C., Rinfret, A., Addison, W. R., Fischer, K. P., Churchill, T. A., Lakey, J. R., *et al.* (2001) *Nat. Med.* **7,** 927–933.
15. Meuleman, P., Libbrecht, L., De Vos, R., de Hemptinne, B., Gevaert, K., Vandekerckhove, J., Roskams, T. & Leroux-Roels, G. (2005) *Hepatology* **41,** 847–856.
16. Major, M. E., Dahari, H., Mihalik, K., Puig, M., Rice, C. M., Neumann, A. U. & Feinstone, S. M. (2004) *Hepatology* **39,** 1709–1720.
17. Thimme, R., Bukh, J., Spangenberg, H. C., Wieland, S., Pemberton, J., Steiger, C., Govindarajan, S., Purcell, R. H. & Chisari, F. V. (2002) *Proc. Natl. Acad. Sci. USA* **99,** 15661–15668.
18. Radaeva, S., Jaruga, B., Kim, W. H., Heller, T., Liang, T. J. & Gao, B. (2004) *Biochem. J.* **379,** 199–208.
19. Bukh, J., Apgar, C. L., Engle, R., Govindarajan, S., Hegerich, P. A., Tellier, R., Wong, D. C., Elkins, R. & Kew, M. C. (1998) *J. Infect. Dis.* **178,** 1193–1197.
20. Hijikata, M., Shimizu, Y. K., Kato, H., Iwamoto, A., Shih, J. W., Alter, H. J., Purcell, R. H. & Yoshikura, H. (1993) *J. Virol.* **67,** 1953–1958.
21. Rueckert, R. R. (1996) in *Fields Virology*, eds. Fields, B. N., Knipe, D. M. & Howley, P. M. (Lippincott-Raven, Philadelphia), Vol. 1, pp. 609–654.
22. Bradley, D., McCaustland, K., Krawczynski, K., Spelbring, J., Humphrey, C. & Cook, E. H. (1991) *J. Med. Virol.* **34,** 206–208.
23. Thomssen, R., Bonk, S., Propfe, C., Heermann, K. H., Kochel, H. G. & Uy, A. (1992) *Med. Microbiol. Immunol. (Berlin)* **181,** 293–300.
24. Bartosch, B., Verney, G., Dreux, M., Donot, P., Morice, Y., Penin, F., Pawlotsky, J. M., Lavillette, D. & Cosset, F. L. (2005) *J. Virol.* **79,** 8217–8229.
25. Meunier, J. C., Engle, R. E., Faulk, K., Zhao, M., Bartosch, B., Alter, H., Emerson, S. U., Cosset, F. L., Purcell, R. H. & Bukh, J. (2005) *Proc. Natl. Acad. Sci. USA* **102,** 4560–4565.
26. Voisset, C., Callens, N., Blanchard, E., Op De Beeck, A., Dubuisson, J. & Vu-Dac, N. (2005) *J. Biol. Chem.* **280,** 7793–7799.
27. Heckel, J. L., Sandgren, E. P., Degen, J. L., Palmiter, R. D. & Brinster, R. L. (1990) *Cell* **62,** 447–456.
28. Meuleman, P., Vanlandschoot, P. & Leroux-Roels, G. (2003) *Biochem. Biophys. Res. Commun.* **308,** 375–378.